



Folic Acid/Peptides Modified PLGA–PEI–PEG Polymeric Vectors as Efficient Gene Delivery Vehicles: Synthesis, Characterization and Their Biological Performance

Chaoyu Liu¹ · Yuancai Xie² · Xiaohua Li¹ · Xumei Yao¹ · Xuanbin Wang^{3,4} · Min Wang⁵ · Zongxian Li⁶ · Fengjun Cao³ 

Accepted: 24 October 2020 / Published online: 3 November 2020
© Springer Science+Business Media, LLC, part of Springer Nature 2020

Abstract

Polymeric vectors are safer alternatives for gene delivery owing to their advantages as compared to viral vectors. To improve the stability and transfection efficiency of poly(lactic-co-glycolic acid) (PLGA)- and poly(ethylenimine) (PEI)-based vectors, poly(ethylene glycol) (PEG), folic acid (FA), arginylglycylaspartic acid (RGD) peptides and isoleucine-lysine-valine-alanine-valine (IKVAV) peptides were employed and PLGA–PEI–PEG–FA and PLGA–PEI–PEG–RGD copolymers were synthesized. PLGA–PEI–PEG–FA/DNA, PLGA–PEI–PEG–RGD/DNA and PLGA–PEI–PEG–RGD/IKVAV/DNA nano-complexes (NCs) were formed through bulk mixing. The structure and properties, including morphology, particle size, surface charge and DNA encapsulation, of NCs were studied. Robust NCs with spherical shape, uniform size distribution and slightly positive charge were able to completely bind DNA above their respective N/P ratios. The critical N/P ratio for PLGA–PEI–PEG–FA/DNA, PLGA–PEI–PEG–RGD/DNA and PLGA–PEI–PEG–RGD/IKVAV/DNA NCs was identified to be 12:1, 8:1 and 10:1, respectively. The covalent modification of PEI through a combination of biodegradable PLGA, hydrophilic PEG and targeting motifs significantly decreased the cytotoxicity of PEI. The developed NCs showed both N/P ratio and cell type-dependent transfection efficiency. An increase in N/P ratio resulted in increased transfection efficiency, and much improved transfection efficiency of NCs was observed above their respective critical N/P ratios. This study provides a promising means to produce polymeric vectors for gene delivery.

Keywords Polymeric vector · Gene delivery · FOLIC acid · RGD peptide · Biocompatibility · Transfection efficiency

Chaoyu Liu and Yuancai Xie have contributed equally.

✉ Zongxian Li
lizongxian66@sina.com

✉ Fengjun Cao
bcsophia@qq.com

¹ Department of Research and Development, Shiningbiotech Co., Ltd, Shenzhen 518055, People's Republic of China

² Department of Thoracic, Peking University Shenzhen Hospital, Shenzhen 518036, People's Republic of China

³ Laboratory of Chinese Herbal Pharmacology, Oncology Center, Renmin Hospital, Hubei University of Medicine, Shiyan 442000, People's Republic of China

⁴ Hubei Key Laboratory of Wudang Local Chinese Medicine Research, Shiyan 442000, People's Republic of China

⁵ Department of Mechanical Engineering, The University of Hong Kong, Pokfulam, Hong Kong, People's Republic of China

⁶ Department of Oncology, Weihai Central Hospital, Weihai, People's Republic of China

Introduction

Owing to the development of cell molecular biology and genetic research in recent years, a number of human diseases have been identified as being triggered by genetic defects and disorders. Gene therapy using deoxyribonucleic acid (DNA) or ribonucleic acid (RNA) as a pharmaceutical agent is considered as the ultimate cure for these genetic diseases. Internalization and utilization of therapeutic genes facilitated by so-called “vectors” into targeted cells in the process of gene delivery are essential and responsible for the success of gene therapy. Compared to viral vectors, polymeric vectors are safer alternatives for gene delivery owing to their advantages including ease of preparation, low cost, structural diversity, manipulable physiochemical properties, vector stability upon storage and reconstitution and larger payload capacity of gene cargo [1]. Although great efforts have been made in recent years to develop various polymeric vectors, very few of them are employed for gene therapy in

clinical applications due to their low transfection efficiency caused by various biological barriers [2–4]. The development of new polymeric vectors with high transfection efficiency and low cytotoxicity is urgently needed.

Various polymers, including biodegradable polymers such as PLGA and polycations such as PEI, have been utilized to construct polymeric vectors for potential applications in gene delivery [5–12]. Knowledge about critical transfection efficiency-limiting barriers, including gene packaging, cellular entry, endo-lysosomal escape, cytosolic transport and nuclear import, DNA/vector dissociation and biostability, has been gained [13]. Different strategies, including PEG modification [14–17], conjugation of targeting ligand such as FA [18–20], and modification by functional peptides such as RGD peptides and IKVAV peptides [21, 22], have been explored to overcome these barriers and improve the transfection efficiency and biocompatibility of designed polymeric vectors.

Polymeric vectors designed through a combinatorial strategy may be advantageous for efficient gene delivery. In order to test this hypothesis, PLGA–PEI–PEG–FA and PLGA–PEI–PEG–RGD copolymers were synthesized through amidation reaction in this project. New polymeric vectors including PLGA–PEI–PEG–FA/DNA, PLGA–PEI–PEG–RGD/DNA and PLGA–PEI–PEG–RGD/IKVAV/DNA NCs were formed through bulk mixing. The structures of synthesized copolymers were characterized by Fourier transform infrared spectroscopy (FTIR). The morphology, particle size and surface charge of different NCs were examined by various characterization techniques. Gel electrophoresis of different DNA complexes at different N/P ratios (molar ratio of amine groups in PEI to phosphate groups in DNA) was conducted to evaluate their DNA encapsulation and condensation efficiency. Cytotoxicity of PLGA–PEI–PEG–FA, PLGA–PEI–PEG–RGD and PLGA–PEI–PEG–RGD/IKVAV and transfection efficiency of their DNA NCs to human embryonic kidney 293 cell line (HEK 293 T) and rat pheochromocytoma cell line (PC12 cells) were assessed.

Materials and Methods

Materials

PLGA (M_w 36 kDa, inherent viscosity 0.2–0.3 dL/g) having a carboxylic group at one end were purchased from Lakeshore Biomaterials, USA. Branched PEI (M_w 25 kDa), PEG (H_2N -PEG-COOH, M_w 2 kDa), folic acid (FA), RGD peptides (Gly-Arg-Gly-Asp-Ser-Pro, GRGDSP) laminin mimetic IKVAV peptides (MAPTRIX-L-IKVAV, M_w 23.1 kDa), N-(3-Dimethylaminopropyl)-N-ethylcarbodiimide hydrochloride (EDC·HCl), N-hydroxy succinimide (NHS) and dialysis tubes (M_w cutoff: 2 kDa and 20 kDa)

were Sigma-Aldrich products. Agarose, loading buffer, Tris–EDTA and ethidium bromide for gel electrophoresis were also purchased from Sigma-Aldrich. Dimethylsulfoxide (DMSO) was supplied by Uni Chem Co., Korea. Alexa Fluor® 594 phalloidin and live/dead cell viability assay kits were purchased from Life Technologies.

Synthesis of Copolymers

PLGA–PEI–PEG–FA and PLGA–PEI–PEG–RGD copolymers were synthesized through amidation reaction as shown in Fig. 1.

PLGA_{36kDa} (0.1 mM) was dissolved in 50 mL of DMSO. To activate the carboxylic groups on the polymer chain, 0.5 mM of EDC·HCl and 0.5 mM of NHS were added into the polymer solution and stirred for 4 h at room temperature. Then 0.1 mM of PEI_{25kDa} dissolved in 50 mL of DMSO was added into the activated polymer solution followed by stirring for 24 h, after which the solution was dialyzed (using dialysis tubing with a M_w cutoff of 20 kDa) against DI water for 48 h and then collected by freeze-drying to obtain PLGA–PEI.

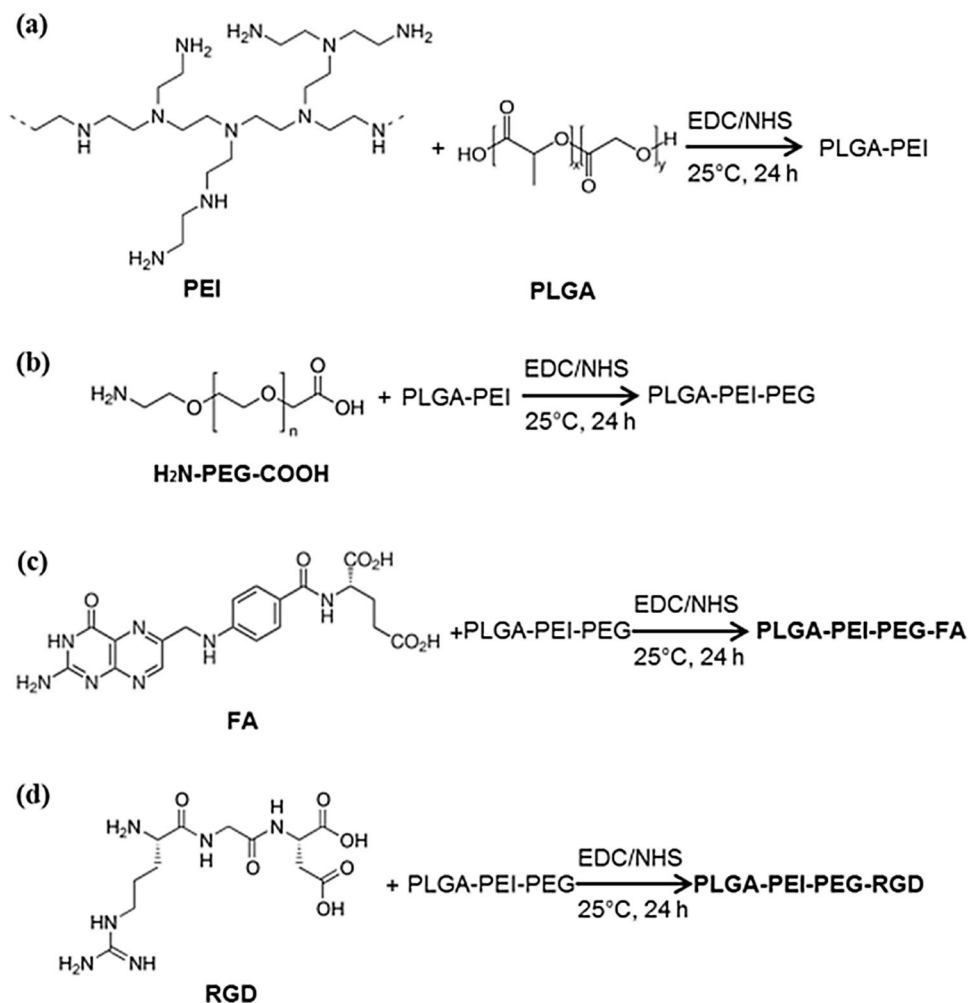
PLGA_{36kDa}–PEI_{25kDa} (0.05 mM) and PEG (0.05 mM) were dissolved in 50 mL of DMSO and 0.25 mM of EDC·HCl and 0.25 mM of NHS were added and stirred for 24 h at room temperature. Then the solution was dialyzed (using dialysis tubing with a M_w cutoff of 2 kDa) against DI water for 48 h and then collected by freeze-drying to obtain PLGA–PEI–PEG.

FA (0.02 mM) was dissolved in 20 mL of DMSO and activated by 0.1 mM of EDC·HCl and 0.1 mM of NHS for 4 h. PLGA–PEI–PEG (0.02 mM) dissolved in 20 mL of DMSO was added to the activated solution and stirred for 24 h at room temperature. Then the solution was dialyzed (using dialysis tubing with a M_w cutoff of 2 kDa) against DI water for 48 h and then collected by freeze-drying to obtain PLGA–PEI–PEG–FA.

RGD peptides (0.02 mM) was dissolved in 20 mL DI water and activated by 0.1 mM of EDC·HCl and 0.1 mM of NHS for 4 h. PLGA–PEI–PEG (0.02 mM) dissolved in 20 mL of DMSO was added to the activated solution and stirred for 24 h at room temperature. Then the solution was dialyzed (using dialysis tubing with a M_w cutoff of 2 kDa) against DI water for 48 h and then collected by freeze-drying to obtain PLGA–PEI–PEG–RGD.

Characterization of Copolymers

The synthesized PLGA–PEI, PLGA–PEI–PEG–RGD and PLGA–PEI–PEG–FA copolymers were analyzed using Fourier transform infrared (FTIR) spectroscopy. KBr tablets were made from a mixture of 2 mg of a copolymer and

Fig. 1 Synthesis of copolymers

0.4 g of KBr powder. The FTIR spectrum of each sample was then obtained using a PerkinElmer® Spectrum BX FTIR System.

Formation of DNA Complexes

Plasmid enhanced green fluorescent protein (pEGFP) with an absorbance_{260nm}/absorbance_{280nm} ratio of 1.88 was obtained through the general preparation method including transformation, propagation and purification using *Escherichia coli* (*E-coli*) provided by Department of Pathology, The University of Hong Kong. DNA complexes were formed through bulk mixing method. Plasmid DNA (pDNA) was diluted to 0.1 mg/mL. An appropriate amount of each nanoparticle solution or copolymer solution was added into the plasmid solution at various N/P ratios and vortexed for 30 s, followed by 30 min incubation at room temperature to obtain various DNA complexes. The N/P ratio was defined as molar ratio of nitrogen in amine groups of PEI to phosphate in DNA.

Morphology and Structure of NCs

Morphological and structural characterization of various fabricated NCs was conducted. Solution of NCs was dripped on silicon wafers or copper grids covered with carbon film and then freeze-dried. The samples of NCs were sputtered with a thin gold coating for 30 s by a sputter coater (BEL-TAC SCD005) and their morphology was examined using SEM (Hitachi S-4800 FEG SEM, Japan). Collected samples of NCs were examined using TEM (Philips EM208s TEM, Netherlands).

Particle Size and Zeta Potential of NCs

The hydrodynamic particle size (by dynamic light scattering) and surface charge of NCs were measured using a particle analyzer (Beckman Coulter Delsa Nano C). NCs were suspended in DI water at appropriate concentrations and their particle size and surface charge were measured at 25° C. At least three replicates were tested for each type of NCs and results were expressed as mean ± SD.

Gel Electrophoresis of NCs

The electrophoretic mobility of prepared DNA complexes with different N/P ratios was evaluated by agarose gel electrophoresis. 2 μL of loading buffer was added to each sample of NCs. Then 5 μL of each sample solution was loaded into wells of 1% agarose gel. The electrophoresis was carried out at 80 V for 30 min in Tris–EDTA buffer. After the completion of electrophoresis, the gels were stained with ethidium bromide (0.5 $\mu\text{g}/\text{mL}$) in Tris–EDTA buffer for 30 min and then rinsed with DI water for 20 min. The DNA bands were visualized with a UV illuminator.

Cell Culture

HEK 293 T cell line used was a human embryonic kidney cell line. PC12 cells were purchased from Biowit Technologies (Shenzhen, China). HEK 293 T and PC12 cells were used for determining the cytotoxicity of fabricated copolymers and transfection efficiency of NCs. Cells were cultured in DMEM culture medium supplemented with glucose (2 g/L), 10% FBS and 1% P/S antibiotics at 37 °C in humidified air containing 5% CO_2 in all experiments. When the cells cultured in a flask achieved 80% confluence, they were enzymatically digested by 0.25% (w/v) trypsin–EDTA from the culture flask, and counted using a haemocytometer for further experiments.

Cytotoxicity of copolymers

In vitro cytotoxicity tests for PEI, PLGA–PEI, PLGA–PEI–PEG–FA, PLGA–PEI–PEG–RGD and PLGA–PEI–PEG–RGD/IKVAV to both types of cells were performed using live/dead assay. Cells were seeded at initial density of 2×10^4 cells/well in 500 μL of growth medium in 24-well plates and incubated in a 5% CO_2 humidified atmosphere at 37 °C for 24 h to reach 80% confluences. Growth media were then replaced by fresh medium which contained various amounts of polymers. Cells were incubated for another 24 h and then treated with 100 μL of live/dead staining solution. The fluorescence for live cells (green) and dead cells (red) was detected with a fluorescence microscope (Nikon Eclipse TE2000-U). The cell viability was calculated using the equation as below:

$$\text{Cell viability (\%)} = \times 100\% \quad (1)$$

In vitro Transfection

In vitro transfection tests for PEI/DNA, PLGA–PEI/DNA, PLGA–PEI–PEG–FA/DNA, PLGA–PEI–PEG–RGD/

DNA and PLGA–PEI–PEG–RGD/IKVAV/DNA NCs to both types of cells at various N/P ratios (5, 8, 10, 12 and 16) were performed. Cells were seeded at initial density of 1×10^4 cells/well in 500 μL of growth medium in 24-well plates and incubated in a 5% CO_2 humidified atmosphere at 37 °C for 24 h. The culture medium was then replaced by fresh medium which contained various amounts of NCs. The pDNA amount in each well was maintained at 5 μg . Cells were incubated for another 24 h, washed twice with PBS and fixed with 4% PFA for 10 min at room temperature. After washing twice with PBS, the cells were permeabilized with 0.1% Triton X-100 solution and incubated in (1% w/v) BSA block solution for 30 min, followed by the incubation in solution containing Alexa Fluor® 594 phalloidin (1:40 dilution) for 30 min for the staining of F-actin. Fluorescence for EGFP (green) and F-actin (red) were detected with a fluorescence microscope. The transfection efficiency was calculated using the equation as below:

$$\text{Transfection efficiency (\%)} = \times 100\% \quad (2)$$

where EGFP-expressing cells were taken as transfected cells.

Results

Synthesis of PLGA–PEI–PEG–FA and PLGA–PEI–PEG–RGD Copolymers

PLGA–PEI copolymer was first synthesized through amidation reaction between PLGA with one carboxyl end group and PEI with amine groups (Fig. 1). FA or RGD was then covalently linked to PLGA–PEI through a bifunctional PEG spacer (HOOC-PEG-NH_2) to synthesize PLGA–PEI–PEG–FA and PLGA–PEI–PEG–RGD copolymers (Fig. 1). The FTIR spectrum of PEI, PLGA, PLGA–PEI, PLGA–PEI–PEG–FA and PLGA–PEI–PEG–RGD is illustrated in Fig. 2. The absorbance at 1573 and 3330 cm^{-1} was detected in PLGA–PEI copolymer attributed to vibration of N–H bond. The absorbance at 2851 and 2929 cm^{-1} was due to vibration of C–H bond and absorbance at 1759 cm^{-1} was caused by stretching of C=O bond in ester group. The obvious absorbance at 1628 cm^{-1} attributed to C=O bond in amide group was also detected in both PLGA–PEI and PLGA–PEI–PEG–FA. A weak absorbance at 1460 and 1560 cm^{-1} attributed to stretching vibration of C=C bond in aromatic ring was detected in PLGA–PEI–PEG–FA copolymer. A wide band absorbance at 1636 cm^{-1} attributed to C=O bond in amide group was observed in PLGA–PEI–PEG–RGD copolymer. The FTIR spectrum confirmed the successful synthesis of PLGA–PEI–PEG–FA and PLGA–PEI–PEG–RGD copolymers.

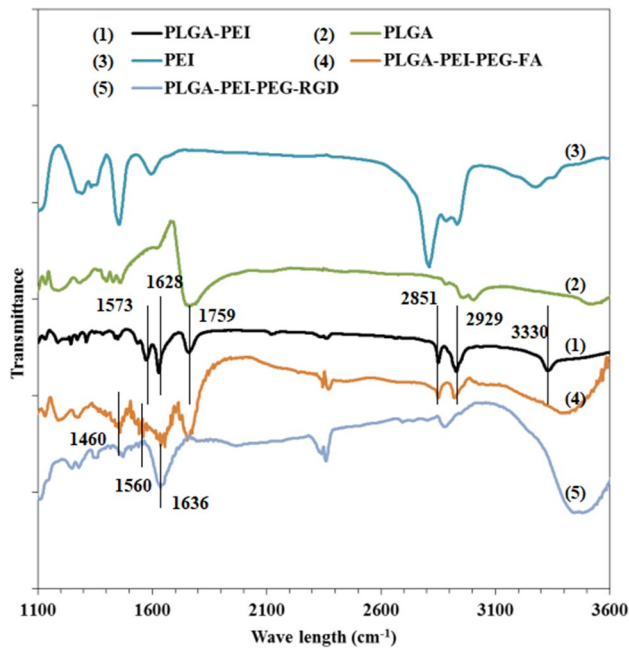


Fig. 2 FTIR spectrum of different polymers

Morphology, Particle Size and Surface Charge of Different NCs

The PEI/DNA, PLGA–PEI–PEG–FA/DNA, PLGA–PEI–PEG–RGD/DNA and PLGA–PEI–PEG–RGD/IKVAV/DNA complexes were formed through bulk mixing with different N/P ratios. The molar ratio of RGD to IKVAV in PLGA–PEI–PEG–RGD/IKVAV/DNA complexes was maintained at 1:1. The morphology of different DNA complexes with 12:1 N/P ratio was examined under both SEM and TEM and is shown in Figs. 3 and 4. The particle size and surface charge of different DNA complexes with different N/P ratios are shown in Fig. 5.

Individual PEI/DNA, PLGA–PEI–PEG–FA/DNA, PLGA–PEI–PEG–RGD/DNA and PLGA–PEI–PEG–RGD/IKVAV/DNA NCs with relatively narrow size distribution were clearly observed under SEM (Fig. 3). The PLGA–PEI–PEG–FA/DNA, PLGA–PEI–PEG–RGD/DNA and PLGA–PEI–PEG–RGD/IKVAV/DNA NCs with diameters less than 200 nm under TEM showed spherical shape without any fusion or agglomeration (Fig. 4). The PEI/DNA polyplexes showed agglomeration to certain extent but had much smaller particle size as compared to other DNA NCs.

The particle size of different DNA NCs with different N/P ratios was measured by dynamic light scattering (DLS) and is shown in Fig. 5a. The particle size of PEI/DNA NCs increased from 89.2 to 128.5 nm as N/P ratio increased from 5:1 to 12:1. The particle size of PLGA–PEI–PEG–FA/DNA NCs decreased from 464.5 to

257.2 nm as N/P ratio increased from 5:1 to 12:1. The particle size of PLGA–PEI–PEG–RGD/DNA NCs decreased from 284.3 to 214.6 nm as N/P ratio increased from 5:1 to 8:1. However, an increase of particle size with the increase of N/P ratio was noticed above 8:1 N/P ratio. Similarly, the particle size of PLGA–PEI–PEG–RGD/IKVAV/DNA NCs decreased from 370.6 to 248.8 nm as N/P ratio increased from 5:1 to 10:1, but increased to 269.9 nm as N/P ratio went up to 12:1. In general, PEI/DNA NCs had the smallest particle size and PLGA–PEI–PEG–FA/DNA NCs showed the largest particle size. The ternary PLGA–PEI–PEG–RGD/IKVAV/DNA NCs incorporated with IKVAV showed increased particle size as compared to PLGA–PEI–PEG–RGD/DNA NCs.

The zeta potential of all NCs increased with the increase of N/P ratio. PEI/DNA NCs showed much higher zeta potential as compared to other NCs. PLGA–PEI–PEG–FA/DNA, PLGA–PEI–PEG–RGD/DNA and PLGA–PEI–PEG–RGD/IKVAV/DNA NCs were all slightly negatively charged at 5:1 N/P ratio but positively charged at 12:1 N/P ratio. PLGA–PEI–PEG–FA/DNA, PLGA–PEI–PEG–RGD/DNA and PLGA–PEI–PEG–RGD/IKVAV/DNA NCs showed a charge reversion at 12:1, 8:1 and 10:1 N/P ratio, respectively.

Gel Electrophoresis of NCs

The gel electrophoresis of different DNA complexes at N/P ratios ranging from 1:1 to 16:1 was conducted and is shown in Fig. 6. The gel electrophoresis pattern showed that PEI, PLGA–PEI, PLGA–PEI–PEG–FA, PLGA–PEI–PEG–RGD and PLGA–PEI–PEG–RGD/IKVAV were able to completely bind DNA above N/P ratio at 4:1, 16:1, 12:1, 8:1 and 10:1, respectively. At lower N/P ratios, free DNA was detected.

Cytotoxicity

The live/dead staining fluorescent images of HEK 293 T and PC12 cells cultured with medium containing different polymers at 100 $\mu\text{g/ml}$ polymer concentration for 1 day are shown in Figs. 7 and 8. The cytotoxicity of PEI, PLGA–PEI–PEG–FA, PLGA–PEI–PEG–RGD and PLGA–PEI–PEG–RGD/IKVAV to HEK 293 T and PC12 cells was evaluated in the dose range that was used in the transfection studies and is shown in Fig. 9.

The live/dead staining fluorescent images (Fig. 7) showed that PEI had much higher cytotoxicity to HEK 293 T cells as compared with other copolymers as many dead cells (stained in red) were observed. The living cells (stained in green) cultured with PEI (Fig. 7a) showed much less green fluorescence intensity, indicating a much lower cell activity, as compared to cells cultured with other copolymers. PLGA–PEI–PEG–FA, PLGA–PEI–PEG–RGD and PLGA–PEI–PEG–RGD/IKVAV showed very little

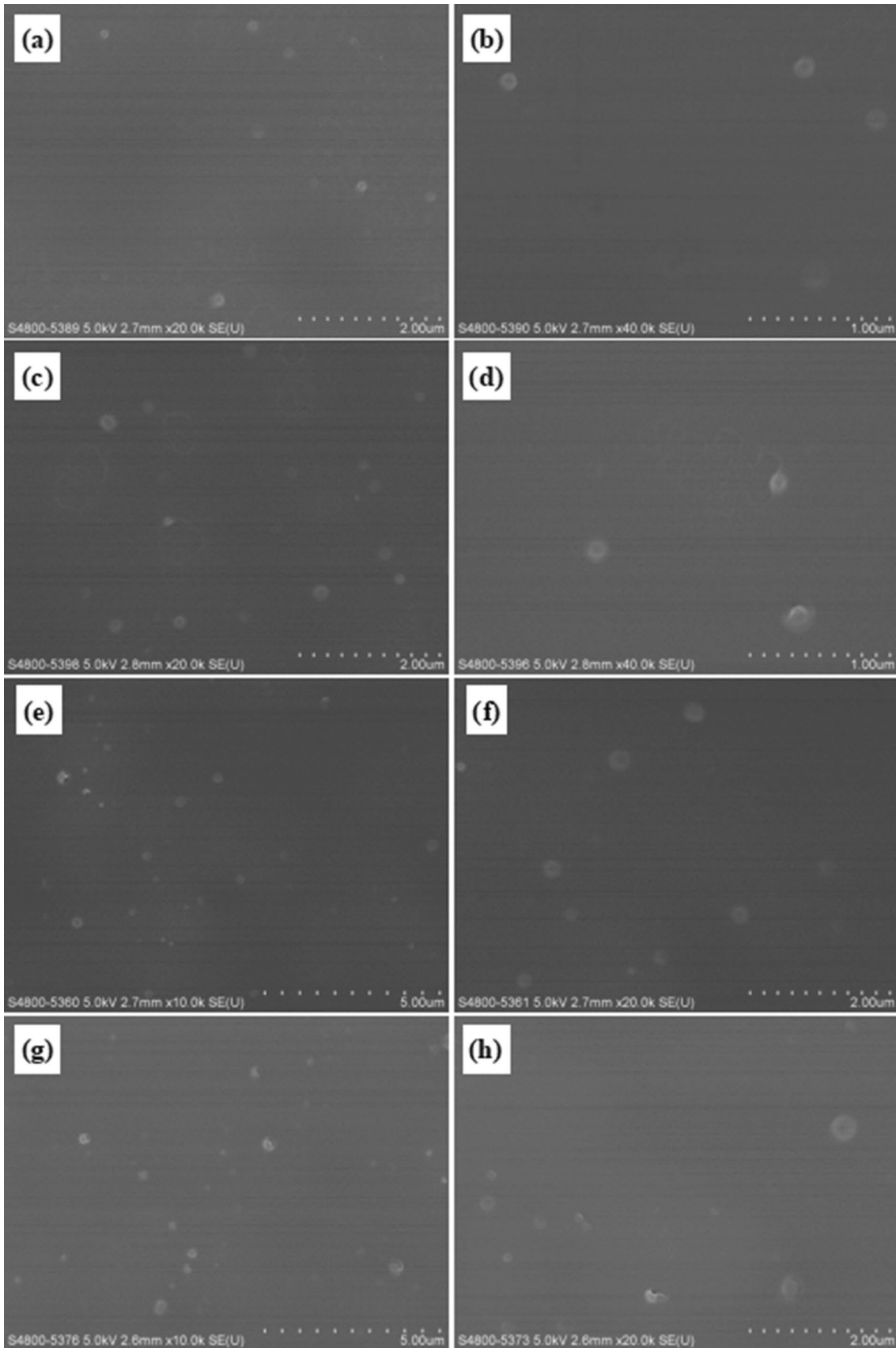


Fig. 3 SEM images of different NCs at 12:1 N/P ratio fabricated by bulk mixing method: **a** and **b** PEI/DNA NCs; **c** and **d** PLGA–PEI–PEG–FA/DNA NCs; **e** and **f** PLGA–PEI–PEG–RGD/DNA NCs; **g** and **h** PLGA–PEI–PEG–FA/IKVAV/DNA NCs

cytotoxicity to HEK 293 T cells as very few dead cells were noticed. Similarly, PEI showed much higher cytotoxicity to PC12 cells as compared with other copolymers as much more cell death was observed (Fig. 8). The much less green fluorescence intensity observed in cells cultured with PEI indicated a lower cell activity. In contrast, PLGA–PEI–PEG–FA, PLGA–PEI–PEG–RGD and PLGA–PEI–PEG–RGD/IKVAV showed much less cytotoxicity to PC12 cells as a small number of dead cells were observed. Interestingly, co-localization of green and red fluorescent signals was observed within both HEK 293 T and PC12 cells cultured with PEI, but not in cells cultured with other copolymers.

The cytotoxicity of PEI, PLGA–PEI–PEG–FA, PLGA–PEI–PEG–RGD and PLGA–PEI–PEG–RGD/IKVAV at different polymer concentrations is shown in Fig. 9. In general, a very similar cytotoxicity to HEK 293 T and PC12 cells was found. PEI showed much higher cytotoxicity to both types of cells at all concentrations as compared to other copolymers. An apparent dose-dependent cytotoxicity of PEI was observed as the cell viability decreased sharply with the increase of PEI concentration. PLGA–PEI–PEG–FA and PLGA–PEI–PEG–RGD showed very little cytotoxicity to both types of cells at polymer concentration below 50 µg/ml. A slight increase of cytotoxicity was noticed at polymer concentration above 100 µg/ml. PLGA–PEI–PEG–RGD/IKVAV showed slightly higher cytotoxicity as compared with the other two types of copolymers. Nevertheless, PLGA–PEI–PEG–FA, PLGA–PEI–PEG–RGD and PLGA–PEI–PEG–RGD/IKVAV showed much improved biocompatibility with both types of cells as compared to PEI.

Transfection Efficiency

The PLGA–PEI–PEG–FA/DNA, PLGA–PEI–PEG–RGD/DNA and PLGA–PEI–PEG–RGD/IKVAV/DNA complexes were formed through bulk mixing with different N/P ratios. The transfection ability of these DNA complexes to HEK 293 T and PC12 cells was evaluated comparing with PEI/DNA polyplexes using pDNA encoding green fluorescent protein as reporter genes. The fluorescent images of HEK 293 T and PC12 cells transfected with different DNA complexes with 12:1 N/P ratio are shown in Figs. 10 and 11, respectively. It was found that all DNA NCs were able to successfully transfect HEK 293 T cells as revealed by green fluorescent signals due to GFP expression (Fig. 10). More GFP-expressing cells

were observed in PLGA–PEI–PEG–FA/DNA (Fig. 10d–f), PLGA–PEI–PEG–RGD/DNA (Fig. 10g–i) and PLGA–PEI–PEG–RGD/IKVAV/DNA (Fig. 10j–l) groups as compared to that in PEI/DNA group (Fig. 10a–c). All DNA NCs were also able to transfect PC12 cells as revealed by GFP expression (Fig. 11). More GFP-expressing cells were observed in PLGA–PEI–PEG–RGD/DNA (Fig. 11g–i) and PLGA–PEI–PEG–RGD/IKVAV/DNA (Fig. 11j–l) groups as compared to that in PEI/DNA group (Fig. 11a–c). However, less GFP-expressing cells were found in PLGA–PEI–PEG–FA/DNA (Fig. 11d–f) group as compared to that in PEI/DNA group.

The transfection efficiency of different DNA complexes with N/P ratio ranging from 5:1 to 12:1 to both types of cells was compared and is shown in Fig. 12. The transfection efficiency was determined by calculating the GFP-expressing cells. The transfection efficiency of PEI/DNA, PLGA–PEI–PEG–FA/DNA, PLGA–PEI–PEG–RGD/DNA and PLGA–PEI–PEG–RGD/IKVAV/DNA NCs to HEK 293 T cells increased from 14.7 to 17.3%, 4.8 to 22.3%, 11.2 to 19.3% and 4.6 to 21.0%, respectively, as N/P ratio increased from 5:1 to 12:1 (Fig. 12a). PLGA–PEI–PEG–FA/DNA, PLGA–PEI–PEG–RGD/DNA and PLGA–PEI–PEG–RGD/IKVAV/DNA NCs showed higher transfection efficiency as compared to PEI/DNA NCs at N/P ratio of 12:1, 8:1 and 10:1, respectively. A sharp increase of transfection efficiency of PLGA–PEI–PEG–FA/DNA, PLGA–PEI–PEG–RGD/DNA and PLGA–PEI–PEG–RGD/IKVAV/DNA NCs was also noticed when the N/P ratio increased to 12:1, 8:1 and 10:1, respectively. Above the critical N/P ratios, transfection efficiency of these NCs increased slowly with the increase of N/P ratio.

The transfection efficiency of PEI/DNA, PLGA–PEI–PEG–FA/DNA, PLGA–PEI–PEG–RGD/DNA and PLGA–PEI–PEG–RGD/IKVAV/DNA NCs to PC12 cells increased from 16.8 to 18.3%, 3.8 to 11.6%, 12.3 to 25.6% and 9.4 to 26.8%, respectively, as N/P ratio increased from 5:1 to 12:1 (Fig. 12b). In general, a higher transfection efficiency to PC12 cells was observed as compared to the transfection efficiency to HEK 293 T cells for all NCs except PLGA–PEI–PEG–FA/DNA NCs. PLGA–PEI–PEG–FA/DNA NCs showed much lower transfection efficiency as compared to other NCs at all N/P ratios although their transfection efficiency increased with the increase of N/P ratios. PLGA–PEI–PEG–RGD/DNA and PLGA–PEI–PEG–RGD/IKVAV/DNA NCs showed much higher transfection efficiency as compared to PEI/DNA NCs at N/P ratio of 8:1 and 10:1, respectively. A sharp increase of transfection efficiency of PLGA–PEI–PEG–RGD/DNA and PLGA–PEI–PEG–RGD/IKVAV/DNA NCs was also noticed when the N/P ratio increased to 8:1 and 10:1, respectively. Above the critical

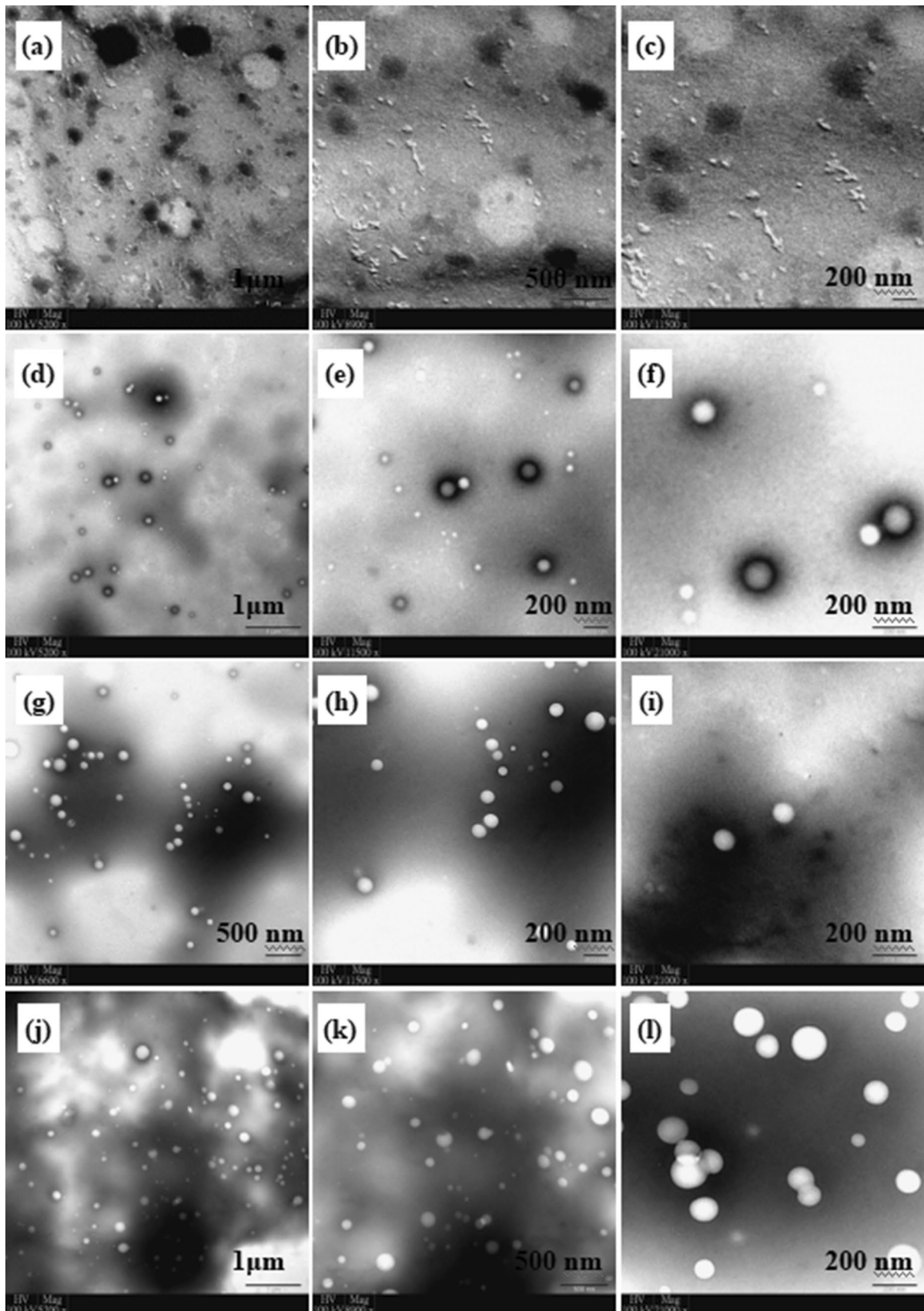


Fig. 4 TEM images of different NCs at 12:1 N/P ratio fabricated by bulk mixing method: **a–c** PEI/DNA NCs; **d–f** PLGA–PEI–PEG–FA/DNA NCs; **g–i** PLGA–PEI–PEG–RGD/DNA NCs; **j–l** PLGA–PEI–PEG–FA/IKVAV/DNA NCs

N/P ratios, transfection efficiency of both types of NCs increased slowly with the increase of N/P ratio.

Discussion

Great efforts have been made to explore polymeric vectors as safe alternatives of viral vectors for gene delivery in recent years. However, limited success in the development of efficient polymeric vectors has been achieved due to their low transfection efficiency. Various strategies have been investigated to improve the transfection efficiency of designed polymeric vectors through overcoming several critical transfection efficiency-limiting barriers [15, 16, 18, 21, 22].

Biocompatible and biodegradable PLGA has been widely utilized in designing polymeric gene delivery vectors owing to their tunable hydrolysis into metabolizable products [14, 23–29]. PEI is well known for its high transfection efficiency but molecular weight-dependent high cytotoxicity [6, 30–32]. The high transfection efficiency is enabled by facilitating endo-lysosomal escape of PEI/DNA polyplexes through a “proton sponge” mechanism [33]. In a recent study by our group, the combination of PLGA and PEI as polymeric vectors through covalent linkage was investigated and expected to overcome the low transfection efficiency of PLGA and high cytotoxicity of PEI. Although PLGA–PEI/DNA NCs showed improved transfection efficiency as compared to naked DNA, their transfection efficiency was much lower as compared to PEI/DNA NCs which was due to their instability in serum-containing medium. The formation of agglomerates of PLGA–PEI/DNA complexes resulted in the difficulty in cellular uptake and hence their very low transfection efficiency. In this study, new polymeric vectors based on PLGA–PEI were designed through a combinatorial strategy. PEG modification of polymeric vectors was intended to improve their hydrophilicity and stability. Conjugation of FA ligand or peptides (RGD or IKVAV peptides) to polymeric vectors was intended to improve their transfection efficiency. The combinatorial strategy was expected to be advantageous for efficient gene delivery.

PLGA–PEI–PEG–FA and PLGA–PEI–PEG–RGD copolymers were synthesized through multi-step amidation reactions using a PEG spacer. Their respective characteristic absorbance bands in FTIR spectrum confirmed the successful synthesis of both types of copolymers (Fig. 2). New polymeric vectors including PLGA–PEI–PEG–FA/DNA, PLGA–PEI–PEG–RGD/DNA and PLGA–PEI–PEG–RGD/IKVAV/DNA NCs were formed through bulk mixing.

Robust PLGA–PEI–PEG–FA/DNA, PLGA–PEI–PEG–RGD/DNA and PLGA–PEI–PEG–RGD/IKVAV/DNA NCs with spherical shape and relatively narrow size distribution were obtained at 12:1 N/P ratio as revealed by their SEM and TEM images (Figs. 3 and 4). All NCs showed diameters less than 200 nm and spherical shape without any fusion or agglomeration (Fig. 4). PEG modification, also called PEGylation, is a useful method to provide hydrophilic shielding, increase stability and ensure prolonged circulation of polymeric vectors [14–17]. It can also serve as active sites for conjugating targeting ligands via covalent bonding [6, 34, 35]. As PEG was much more hydrophilic than PEI and PLGA, it was believed that PEGylation using PEG as a spacer in this study facilitated the formation of a hydrophilic corona and improved the stability and dispersion of PLGA–PEI–PEG–FA/DNA, PLGA–PEI–PEG–RGD/DNA and PLGA–PEI–PEG–RGD/

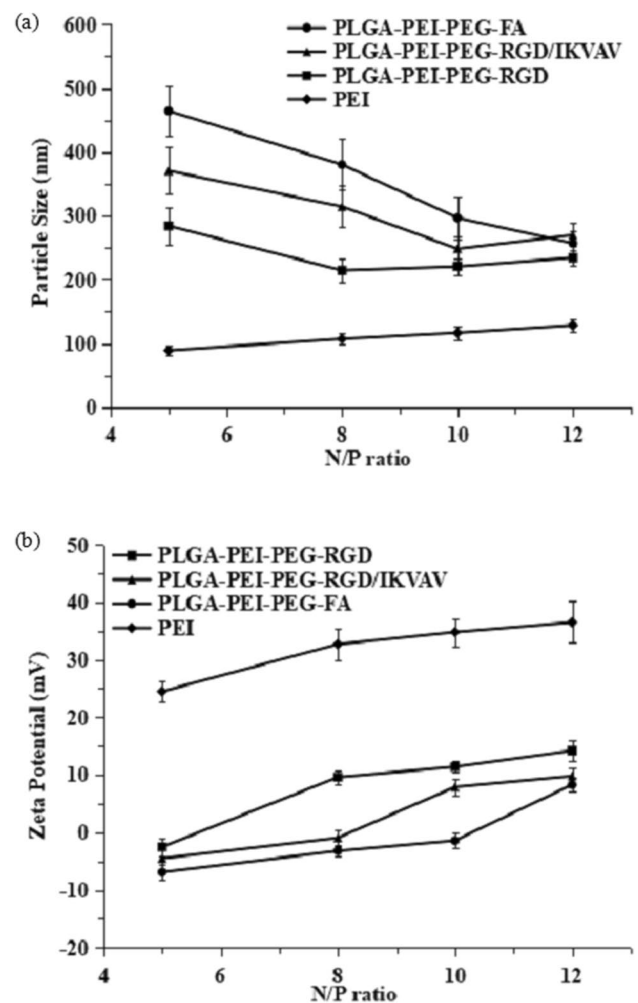
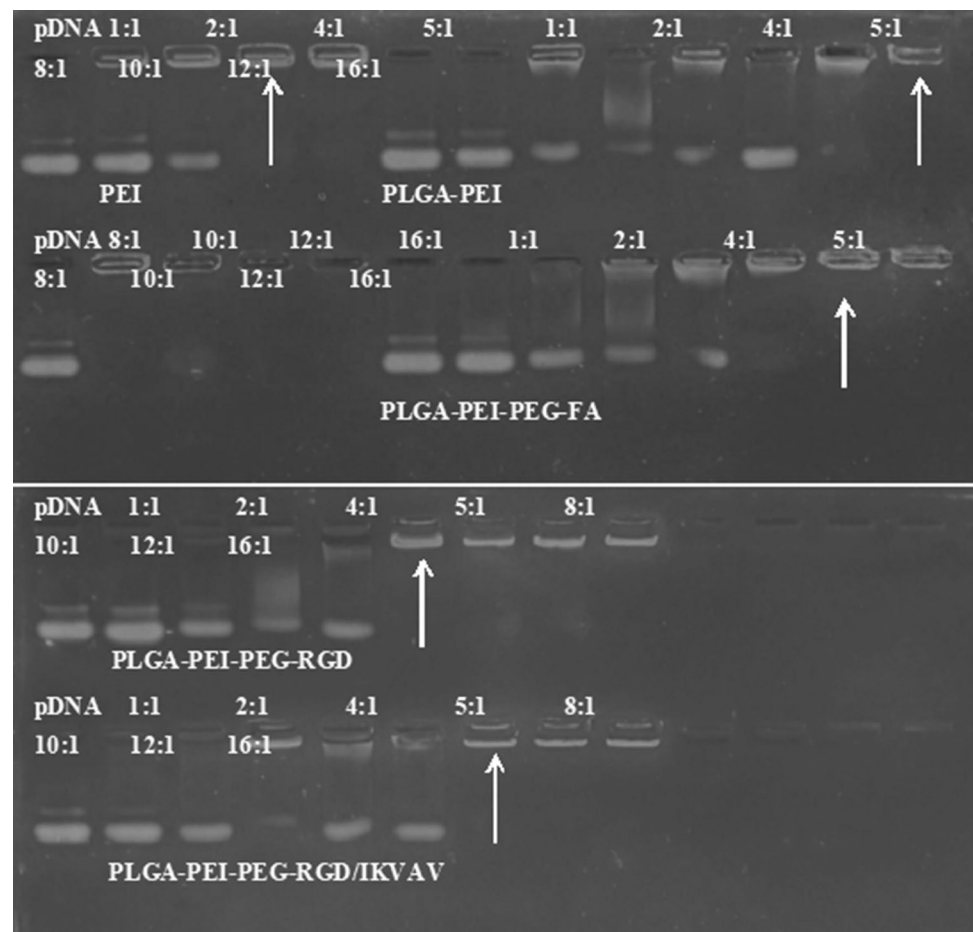


Fig. 5 Particle size and surface charge of different NCs fabricated by bulk mixing: **a** particle size of NCs measured by DLS, **b** zeta potential of NCs

Fig. 6 Gel electrophoresis of PEI/DNA, PLGA–PEI/DNA, PLGA–PEI–PEG–FA/DNA, PLGA–PEI–PEG–RGD/DNA and PLGA–PEI–PEG–RGD/IKVAV/DNA NCs at different N/P ratios



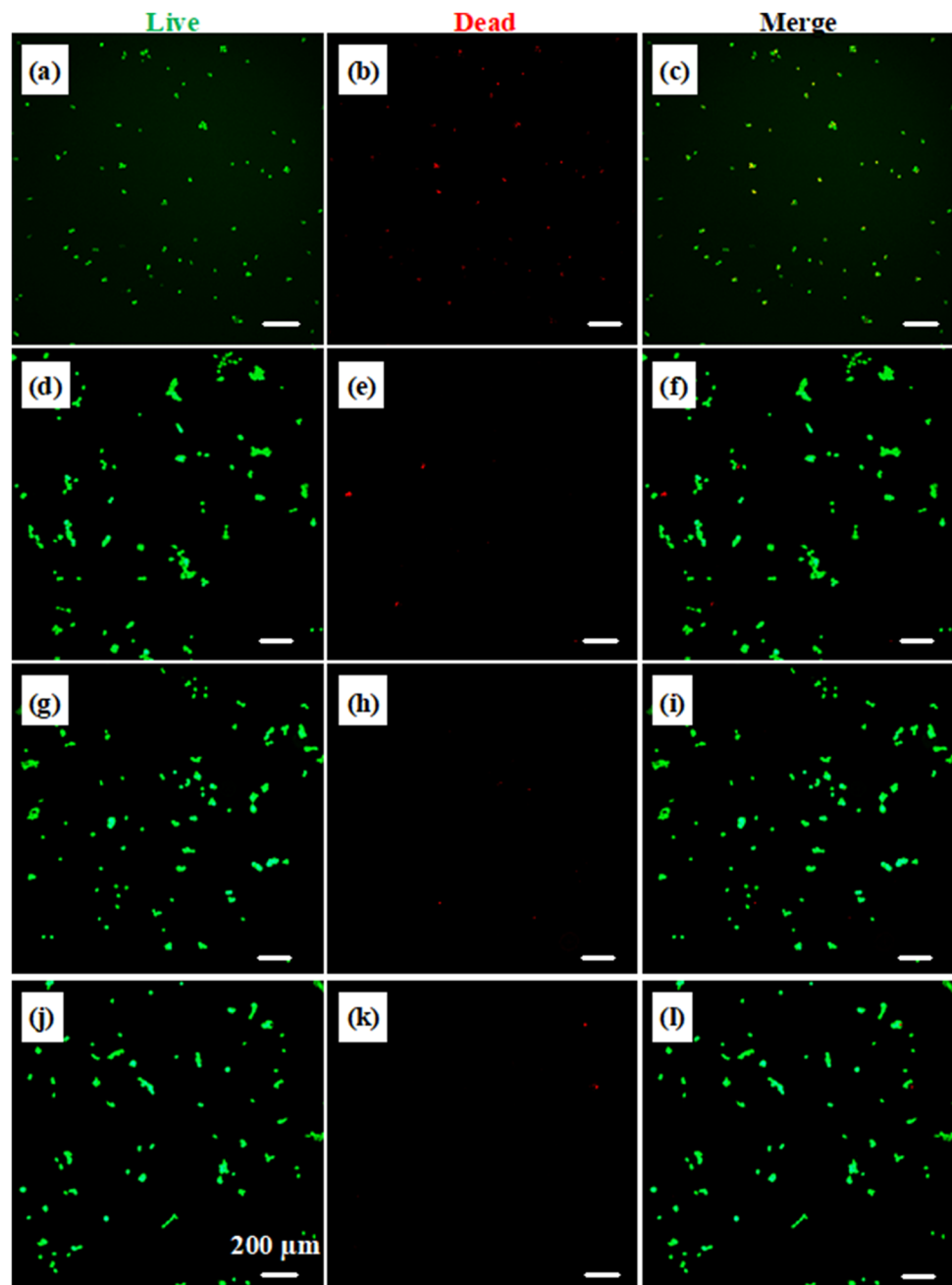
IKVAV/DNA NCs. The PEI/DNA NCs without PEG modification showed partial agglomeration (Fig. 4a–c).

The critical N/P ratio for PLGA–PEI–PEG–FA/DNA, PLGA–PEI–PEG–RGD/DNA and PLGA–PEI–PEG–RGD/IKVAV/DNA NCs to completely encapsulate DNA was identified to be 12:1, 8:1 and 10:1, respectively, as revealed by the gel electrophoresis result (Fig. 6). The results of particle size measured by DLS of NCs at different N/P ratios also confirmed their respective critical N/P ratios. Below the critical N/P ratio, NCs showed a decrease of particle size with the increase of N/P ratio and had a much larger particle size, indicating the formation of agglomeration, as they were not able to completely encapsulate negatively charged DNA through electrostatic interaction below the critical N/P ratio. However, above the critical N/P ratio, NCs fully encapsulated DNA and their particle size increased as the N/P ratio increased. This phenomenon was in consistent with the result of particle size of PEI/DNA NCs. As PEI/DNA NCs were able to fully condense DNA at 4:1 N/P ratio, their particle size slowly increased as the N/P ratio increased from 5:1 to 12:1. The zeta potential of all NCs increased with the

increase of N/P ratio as expected. The observation of charge reversion for different NCs at their respective N/P ratios was in consistent with the results of gel electrophoresis and particle size. Not surprisingly, a suitable N/P ratio was required for NCs to fully encapsulate negatively charged DNA by positively charged copolymers.

PEI/DNA NCs had much smaller particle size but higher surface charge attributed to much lower molecular weight of PEI and much higher content of amine groups as compared to PLGA–PEI based NCs. The PEGylation and conjugation of FA or RGD resulted in a much increase in particle size and decrease in surface charge of NCs as compared to PEI/DNA NCs. RGD peptide is much more hydrophilic than FA and contains amine groups in arginine, which contributed to a decrease in particle size and increase in surface charge of PLGA–PEI–PEG–RGD/DNA NCs as compared to PLGA–PEI–PEG–FA/DNA NCs. The intercalation of amphoteric IKVAV peptides resulted in an increase of particle size and slight decrease of surface charge of ternary PLGA–PEI–PEG–RGD/IKVAV/DNA NCs as compared to PLGA–PEI–PEG–RGD/DNA NCs.

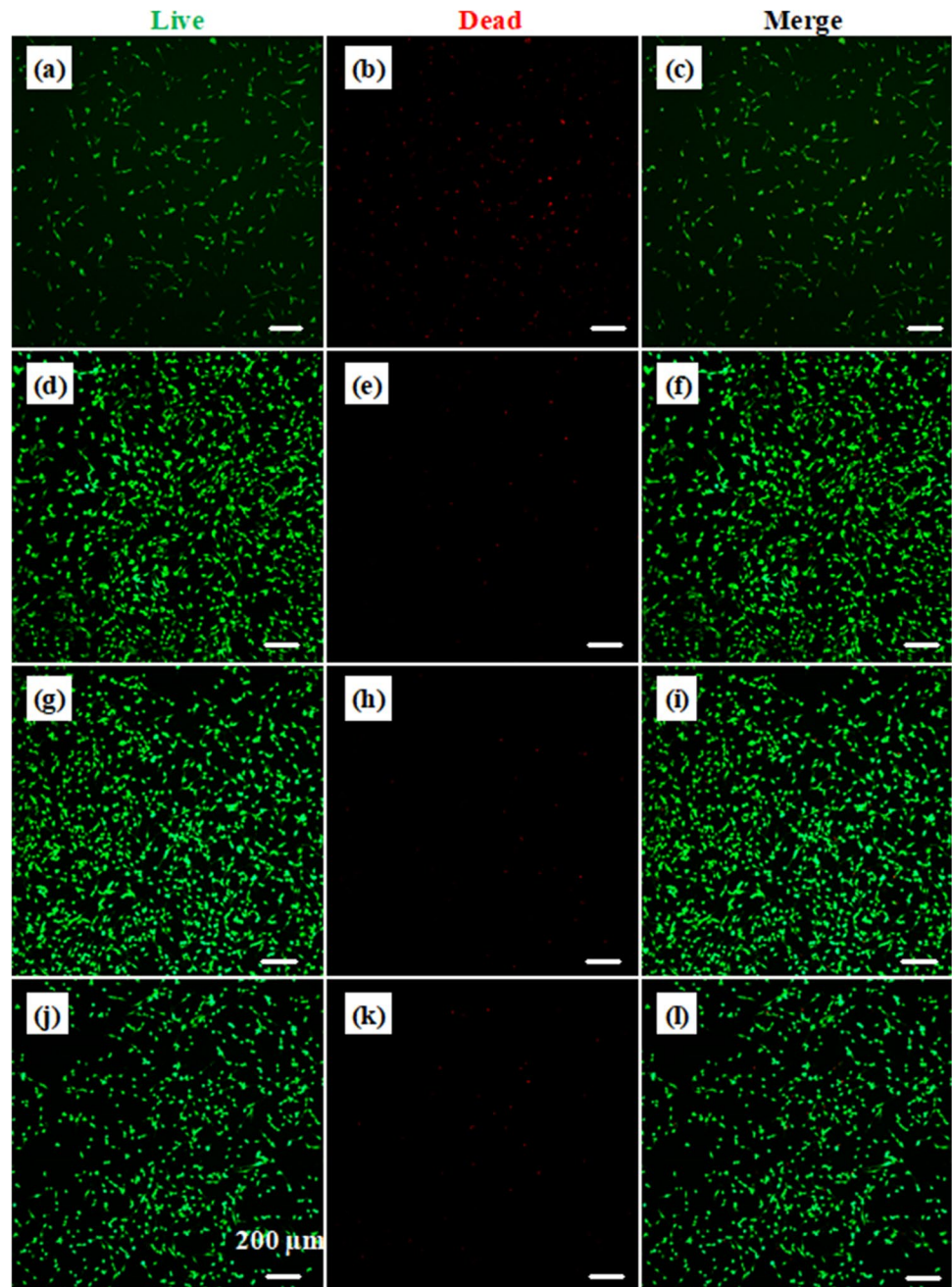
Fig. 7 Live/dead staining of HEK 293 T cells cultured with different polymers at 100 $\mu\text{g}/\text{ml}$ concentration: **a–c** PEI25k; **d–f** PLGA–PEI–PEG–FA copolymer; **g–i** PLGA–PEI–PEG–RGD copolymer; **j–l** PLGA–PEI–PEG–RGD/IKVAV



Although PEGylation provides hydrophilic shielding, improves water solubility, avoids aggregation and prevent opsonization during blood circulation of polymeric vectors, it strongly inhibits cellular uptake and endosomal escape and decreases the transfection activity of polymeric vectors, resulting in a “PEG dilemma” [36, 37]. Folic acid (FA) is a known targeting ligand for most tumors. Covalent conjugation of FA to polymeric vectors could promote their transfection efficiency in FA receptor-overexpressed cells [18–20]. Peptides such as RGD peptides and IKVAV peptides

regulate integrin-mediated cell adhesion [38, 39]. The modification of polymeric vectors by these peptides has also been reported to provide enhanced transfection efficiency [21, 22]. In order to improve the endocytosis of PEGylated NCs and their transfection efficacy, targeting moieties FA or RGD peptide were covalently conjugated to PEGylated copolymers to form PLGA–PEI–PEG–FA/DNA and PLGA–PEI–PEG–RGD/DNA NCs. IKVAV peptides were also intercalated to form ternary PLGA–PEI–PEG–RGD/IKVAV/DNA NCs.

Fig. 8 Live/dead staining of PC12 cells cultured with different polymers at 100 $\mu\text{g}/\text{ml}$ concentration: **a–c** PEI25k; **d–f** PLGA–PEI–PEG–FA copolymer; **g–i** PLGA–PEI–PEG–RGD copolymer; **j–l** PLGA–PEI–PEG–RGD/IKVAV



The cytotoxicity of PEI, PLGA–PEI–PEG–FA, PLGA–PEI–PEG–RGD and PLGA–PEI–PEG–RGD/IKVAV to HEK 293 T and PC12 cells was evaluated through the live/dead staining assay. PEI showed significantly higher cytotoxicity as compared to PLGA–PEI–PEG–FA, PLGA–PEI–PEG–RGD and PLGA–PEI–PEG–RGD/IKVAV and an obvious dose-dependent cytotoxicity of PEI was

observed. The living cells (stained in green) in PEI group (Fig. 7a) showed much less green fluorescence intensity, indicating a much lower cell activity, as compared to cells in other groups. The observed co-localization of green and red fluorescent signals within both HEK 293 T and PC12 cells in PEI group indicated the cell necrosis and apoptosis caused by cytotoxicity of PEI [30]. PLGA–PEI–PEG–FA

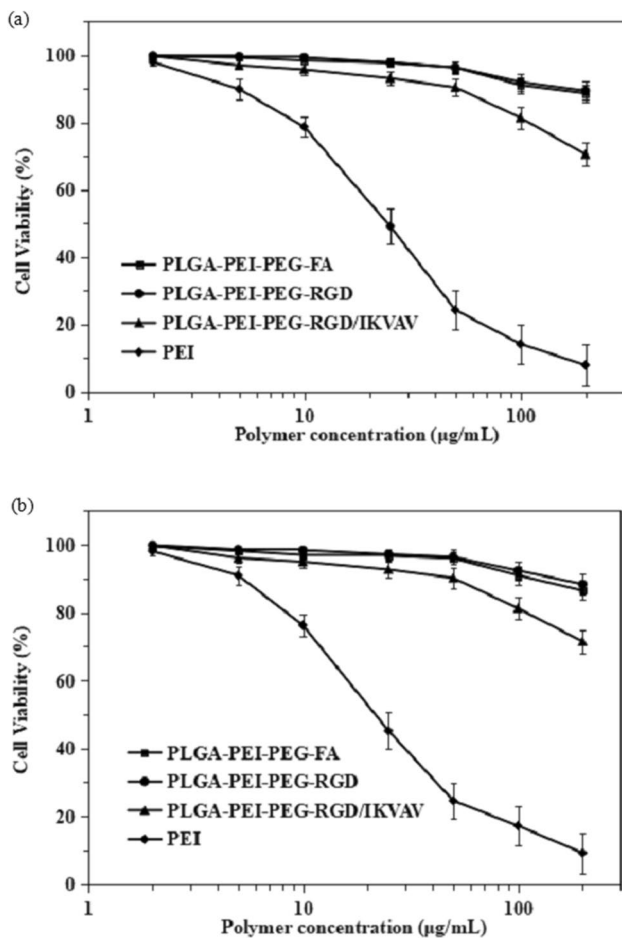


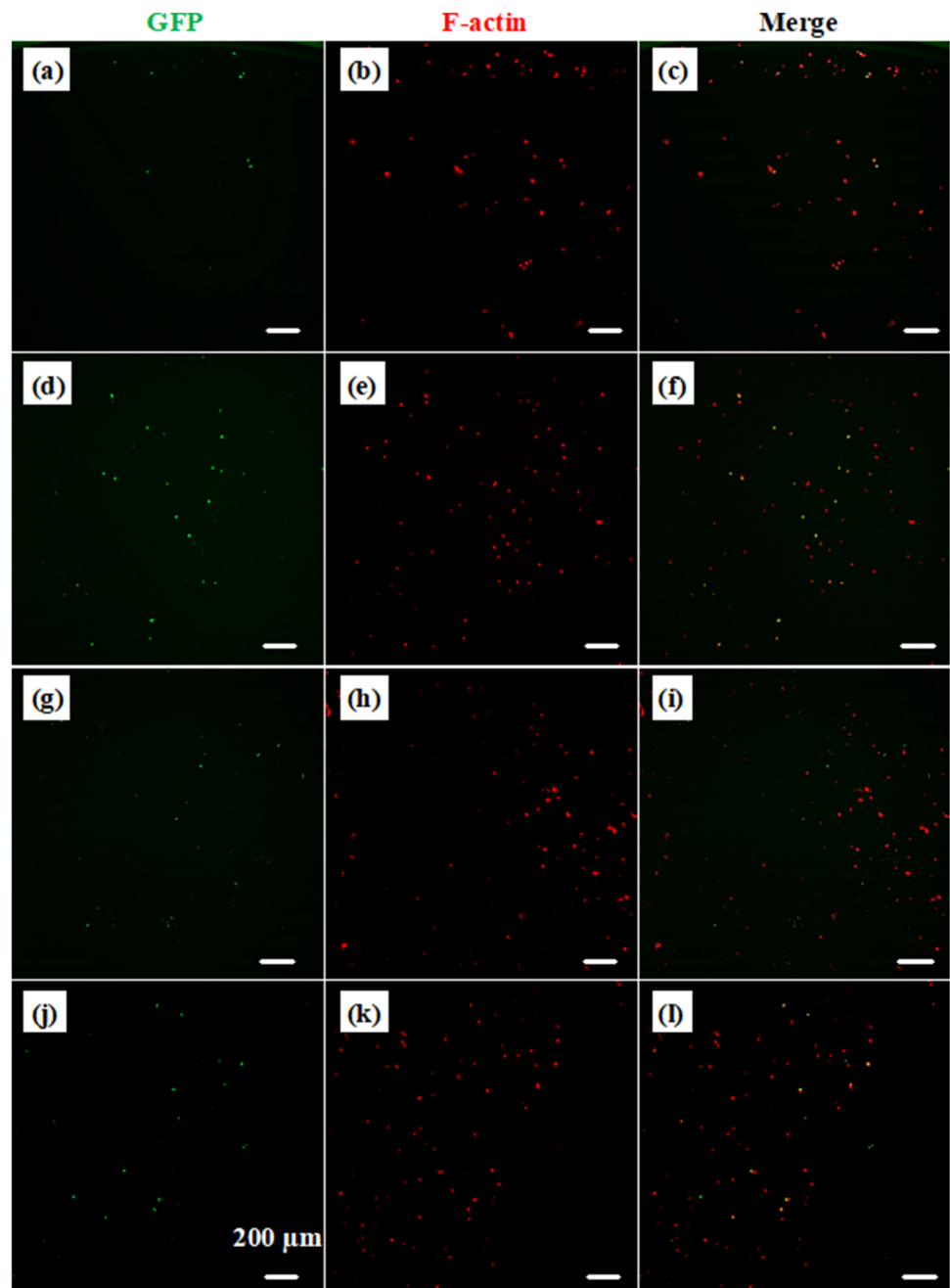
Fig. 9 Cytotoxicity of PEI, PLGA–PEI–PEG–FA copolymer, PLGA–PEI–PEG–RGD copolymer and PLGA–PEI–PEG–RGD/IKVAV to different types of cells: **a** HEK 293 T cells, **b** PC12 cells

and PLGA–PEI–PEG–RGD showed very little cytotoxicity to both types of cells, although a slight increase of cytotoxicity was observed at very high polymer concentration, suggesting that the covalent modification of PEI through a combination of biodegradable PLGA, hydrophilic PEG and targeting motifs significantly decreased the cytotoxicity of PEI. The intercalation of laminin mimetic IKVAV peptides (MW ~ 23 kDa) resulted in a limited increase of cytotoxicity of PLGA–PEI–PEG–RGD/IKVAV as compared to PLGA–PEI–PEG–RGD. Nevertheless, PLGA–PEI–PEG–FA, PLGA–PEI–PEG–RGD and PLGA–PEI–PEG–RGD/IKVAV showed much improved biocompatibility with both HEK 293 T cells and PC12 cells.

The PEI/DNA, PLGA–PEI–PEG–FA/DNA, PLGA–PEI–PEG–RGD/DNA and PLGA–PEI–PEG–RGD/IKVAV/DNA complexes were successfully formed through bulk mixing at different N/P ratios and showed both N/P ratio and cell type-dependent transfection efficiency. All of the DNA complexes were able to transfect both HEK 293 T and PC12 cells as revealed by green fluorescent signals due to GFP expression (Figs. 10 and 11). With the increase of N/P ratio, all DNA complexes showed increased transfection efficiency (Fig. 12). The sharp increase in transfection efficiency of PLGA–PEI–PEG–FA/DNA, PLGA–PEI–PEG–RGD/DNA and PLGA–PEI–PEG–RGD/IKVAV/DNA complexes at their respective critical N/P ratios was attributed to the complete encapsulation and condensation of DNA. Above the critical N/P ratios, transfection efficiency of these NCs increased slowly with the increase of N/P ratio, indicating that additional copolymer would result in very limited increase of transfection efficiency of NCs after the complete encapsulation of DNA. PEI is well known for its high transfection efficiency in gene delivery. PEI with one out of every three atoms of the polymer backbone being nitrogen has high cationic charge potential and can condense and package negatively charged DNA through electrostatic interaction and facilitates its cellular entry and endosomal escape through a “proton sponge” mechanism [31, 32, 34]. PEI/DNA NCs showed higher transfection efficiency at 5:1 N/P ratio as compared to other NCs as PEI/DNA NCs were able to fully condense DNA at 4:1 N/P ratio. However, PLGA–PEI–PEG–FA/DNA NCs showed enhanced transfection efficiency to HEK 293 T cells but lower transfection efficiency to PC12 cells as compared to PEI/DNA NCs at 12:1 N/P ratio. PLGA–PEI–PEG–RGD/DNA and PLGA–PEI–PEG–RGD/IKVAV/DNA NCs showed much improved transfection efficiency to both HEK 293 T and PC12 cells as compared to PEI/DNA NCs above their respective critical N/P ratios. The intercalation of IKVAV peptides in PLGA–PEI–PEG–RGD/IKVAV/DNA NCs improved their transfection efficiency as compared to PLGA–PEI–PEG–RGD/DNA NCs. RGD or IKVAV peptide-modified NCs showed higher transfection efficiency in PC12 cells than in HEK 293 T cells.

FA is a known targeting ligand for many types of cancer cells as the folate receptor (FR) is often over-expressed on the surfaces of these cancer cells [18–20, 40]. It was believed that the FA ligands facilitated the PLGA–PEI–PEG–FA/DNA NCs targeting to the FR of HEK 293 T cells and accumulating on the cell surface, benefiting the cellular uptake

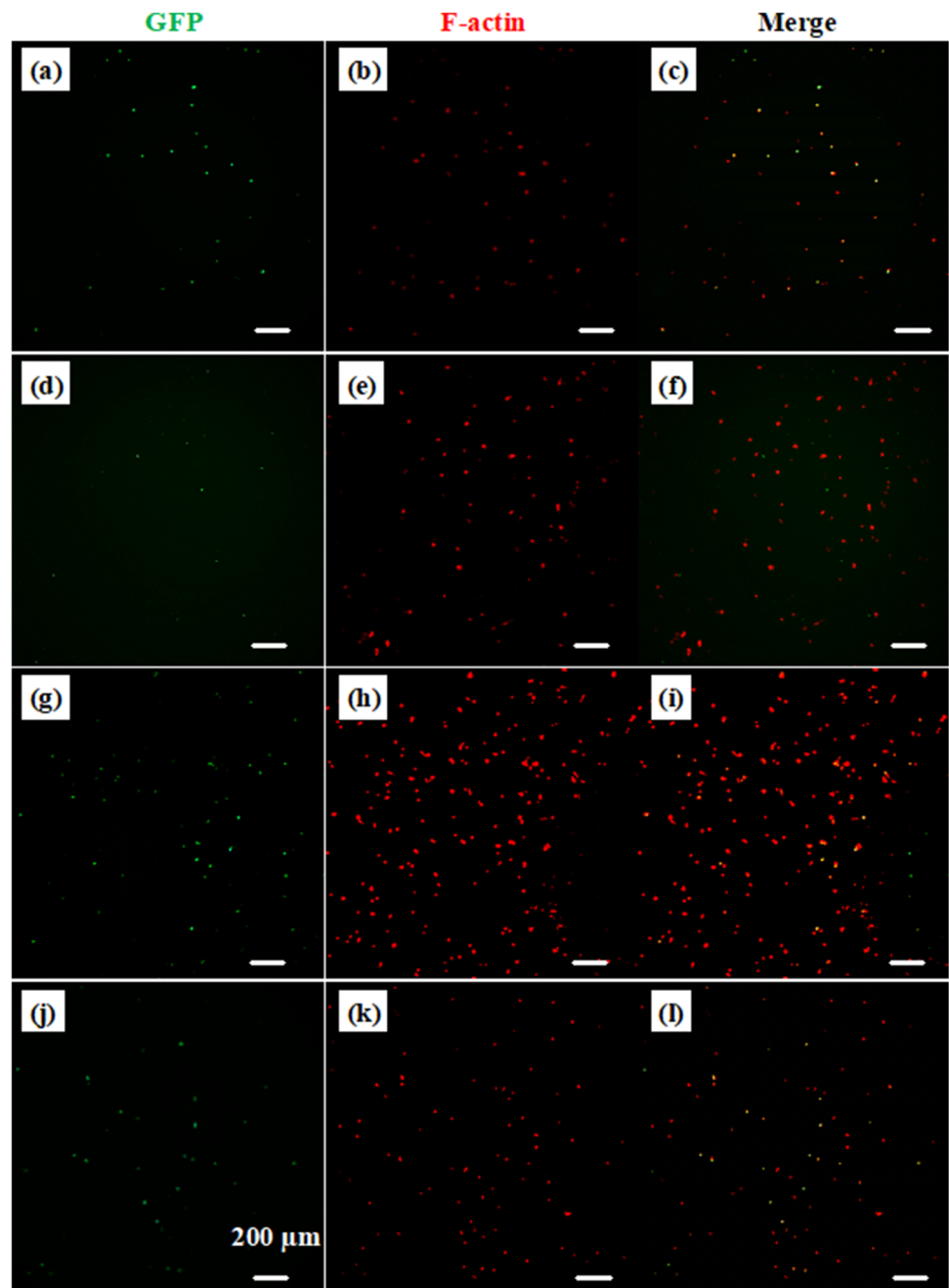
Fig. 10 In vitro transfection of HEK 293 T cells using different DNA complexes at 12:1 N/P ratio: **a–c** PEI25k/DNA complexes; **d–f** PLGA–PEI–PEG–FA/DNA complexes; **g–i** PLGA–PEI–PEG–RGD/DNA complexes; **j–l** PLGA–PEI–PEG–RGD/IKVAV/DNA complexes



of NCs by FR receptor-mediated endocytosis and eventually resulting in a much improved transfection efficiency in HEK 293 T cells. Much lower transfection efficiency was obtained in FR-negative PC12 cells. RGD motif-containing peptides and IKVAV motif-containing peptides are both involved in cell contact interactions through binding to different integrin

receptors and can be used to improve the transfection efficiency of polymeric vectors through integrin-mediated endocytosis [21, 22, 39, 41–43]. Furthermore, IKVAV motif-containing peptides are able to promote neuronal cell adhesion and differentiation [38, 41, 44]. The integrin-mediated endocytosis might result in the much improved

Fig. 11 In vitro transfection of PC12 cells using different DNA complexes at 12:1 N/P ratio: **a–c** PEI25k/DNA complexes; **d–f** PLGA–PEI–PEG–FA/DNA complexes; **g–i** PLGA–PEI–PEG–RGD/DNA complexes; **j–l** PLGA–PEI–PEG–RGD/IKVAV/DNA complexes



transfection efficiency of PLGA–PEI–PEG–RGD/DNA and PLGA–PEI–PEG–RGD/IKVAV/DNA NCs to both types of cells as compared to the “gold standard” PEI/DNA NCs, which was more obvious in PC12 cells which could differentiate into neuron-like cells. The intercalation of IKVAV

peptides in PLGA–PEI–PEG–RGD/IKVAV/DNA NCs provided a synergistic effect on improving their transfection efficiency in both types of cells [45].

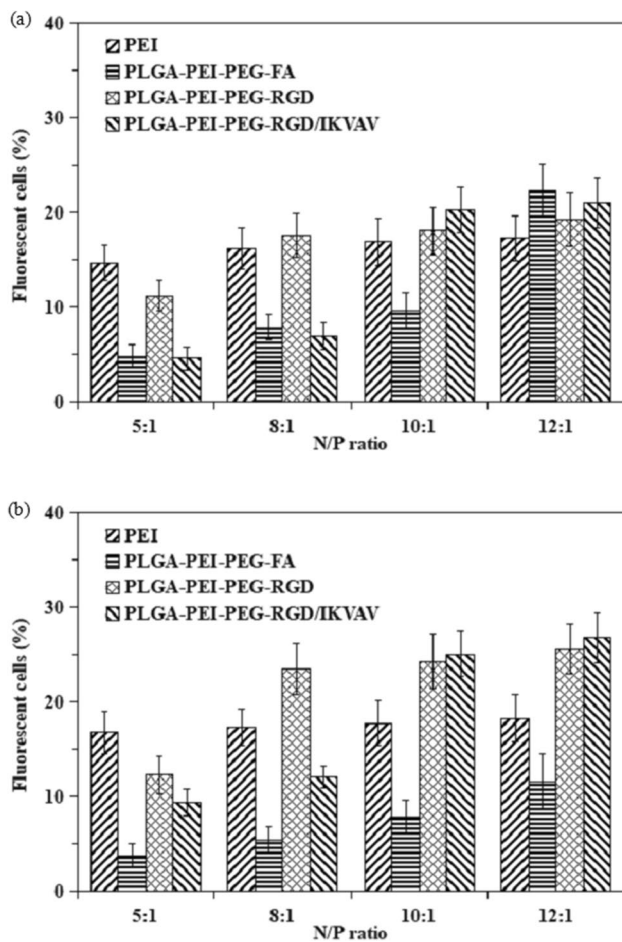


Fig. 12 Transfection efficiency of PEI25k/DNA, PLGA–PEI–PEG–FA/DNA, PLGA–PEI–PEG–RGD/DNA and PLGA–PEI–PEG–RGD/IKVAV/DNA complexes to HEK 293 T cells and PC12 cells

Acknowledgements This work was supported by the Hong Kong Research Grants Council through a GRF grant (Grant No: HKU 718109E); the Guangdong Special Support Plan for High Level Talents of China (Grant No: 2015TQ01R546) and the Hubei Natural Science Foundation of China (Grant No: 2018CFC874).

Compliance with Ethical Standards

Conflict of interest There are no conflicts of interest to declare.

References

- Mastrobattista, E., & Hennink, W. E. (2012). Polymers for gene delivery charged for success. *Nature Materials*, *11*(1), 10–12.
- Putnam, D. (2006). Polymers for gene delivery across length scales. *Nature Materials*, *5*(6), 439–451.
- Zhang, Y., Satterlee, A., & Huang, L. (2012). In vivo gene delivery by nonviral vectors: Overcoming hurdles? *Molecular Therapy*, *20*(7), 1298–1304.
- Martens, T. F., Remaut, K., Demeester, J., De Smedt, S. C., & Braeckmans, K. (2014). Intracellular delivery of nanomaterials: How to catch endosomal escape in the act. *Nano Today*, *9*(3), 344–364.
- Kim, J. H., Park, J. S., et al. (2011). The use of biodegradable PLGA nanoparticles to mediate SOX9 gene delivery in human mesenchymal stem cells (hMSCs) and induce chondrogenesis. *Biomaterials*, *32*(1), 268–278.
- Dai, J. A., Zou, S. Y., Pei, Y. Y., Cheng, D., Ai, H., & Shuai, X. T. (2011). Polyethylenimine-grafted copolymer of poly(L-lysine) and poly(ethylene glycol) for gene delivery. *Biomaterials*, *32*(6), 1694–1705.
- Lai, W.-F. (2014). Cyclodextrins in non-viral gene delivery. *Biomaterials*, *35*(1), 401–411.
- More, H. T., Frezzo, J. A., Dai, J., Yamano, S., & Montclare, J. K. (2014). Gene delivery from supercharged coiled-coil protein and cationic lipid hybrid complex. *Biomaterials*, *35*(25), 7188–7193.
- Tanaka, H., Akita, H., Ishiba, R., et al. (2014). Neutral biodegradable lipid-envelope-type nanoparticle using vitamin A-Scaffold for nuclear targeting of plasmid DNA. *Biomaterials*, *35*(5), 1755–1761.
- Unzueta, U., Saccardo, P., Domingo-Espin, J., et al. (2014). Sheltering DNA in self-organizing, protein-only nano-shells as artificial viruses for gene delivery. *Nanomedicine-Nanotechnology Biology and Medicine*, *10*(3), 535–541.
- Morris, V. B., & Labhasetwar, V. (2015). Arginine-rich polyplexes for gene delivery to neuronal cells. *Biomaterials*, *60*, 151–160.
- Yue, J. H., Wu, J., Liu, D., Zhao, X. L., & Lu, W. W. (2015). BMP2 gene delivery to bone mesenchymal stem cell by chitosan-g-PEI nonviral vector. *Nanoscale Research Letters*, *10*, 203.
- Wong, S. Y., Pelet, J. M., & Putnam, D. (2007). Polymer systems for gene delivery—Past, present, and future. *Progress in Polymer Science (Oxford)*, *32*(8–9), 799–837.
- Wu, G. C., Zhou, F., Ge, L. F., Liu, X. M., & Kong, F. S. (2012). Novel mannan-PEG-PE modified bioadhesive PLGA nanoparticles for targeted gene delivery. *Journal of Nanomaterials*. <https://doi.org/10.1155/2012/981670>
- Shi, S., Shi, K., Tan, L., et al. (2014). The use of cationic MPEG-PCL-g-PEI micelles for co-delivery of Msurvivin T34A gene and doxorubicin. *Biomaterials*, *35*(15), 4536–4547.
- Tagalakakis, A. D., Kenny, G. D., et al. (2014). PEGylation improves the receptor-mediated transfection efficiency of peptide-targeted, self-assembling, anionic nanocomplexes. *Journal of Controlled Release*, *174*, 177–187.
- Yu, J., Deng, H., Xie, F., Chen, W., Zhu, B., & Xu, Q. (2014). The potential of pH-responsive PEG-hyperbranched polyacylhydrazone micelles for cancer therapy. *Biomaterials*, *35*(9), 3132–3144.
- Jiang, Q. Y., Lai, L. H., et al. (2011). Gene delivery to tumor cells by cationic polymeric nanovectors coupled to folic acid and the cell-penetrating peptide octaarginine. *Biomaterials*, *32*(29), 7253–7262.
- Liang, B., He, M. L., Xiao, Z. P., et al. (2008). Synthesis and characterization of folate-PEG-grafted-hyperbranched-PEI for tumor-targeted gene delivery. *Biochemical and Biophysical Research Communications*, *367*(4), 874–880.
- Liang, B., He, M. L., et al. (2009). The use of folate-PEG-grafted-hyperbranched-PEI nonviral vector for the inhibition of glioma growth in the rat. *Biomaterials*, *30*(23–24), 4014–4020.
- Kim, H. A., Nam, K., & Kim, S. W. (2014). Tumor targeting RGD conjugated bio-reducible polymer for VEGF siRNA expressing plasmid delivery. *Biomaterials*, *35*(26), 7543–7552.
- Majzoub, R. N., Chan, C.-L., et al. (2014). Uptake and transfection efficiency of PEGylated cationic liposome-DNA complexes with and without RGD-tagging. *Biomaterials*, *35*(18), 4996–5005.
- Langer, R., & Tirrell, D. A. (2004). Designing materials for biology and medicine. *Nature*, *428*(6982), 487–492.

24. Bordelon, H., Biris, A. S., Sabliov, C. M., & Monroe, W. T. (2011). Characterization of plasmid DNA location within chitosan/PLGA/pDNA nanoparticle complexes designed for gene delivery. *Journal of Nanomaterials*. <https://doi.org/10.1155/2011/952060>
25. Mishra, D., Kang, H. C., & Bae, Y. H. (2011). Reconstitutable charged polymeric (PLGA) (2)-b-PEI micelles for gene therapeutics delivery. *Biomaterials*, 32(15), 3845–3854.
26. Zeng, P., Xu, Y., Zeng, C. H., Ren, H., & Peng, M. L. (2011). Chitosan-modified poly(D, L-lactide-co-glycolide) nanospheres for plasmid DNA delivery and HBV gene-silencing. *International Journal of Pharmaceutics*, 415(1–2), 259–266.
27. Kong, F. S., Ge L. F., Liu X. M., Huang N., & Zhou F. (2012). Mannan-modified PLGA Nanoparticles for targeted gene delivery. *International Journal of Photoenergy*.
28. Tang, J., Chen, J. Y., et al. (2012). Calcium phosphate embedded PLGA nanoparticles: A promising gene delivery vector with high gene loading and transfection efficiency. *International Journal of Pharmaceutics*, 431(1–2), 210–221.
29. Liu, P., Sun, Y., Wang, Q., Sun, Y., Li, H., & Duan, Y. (2014). Intracellular trafficking and cellular uptake mechanism of mPEG-PLGA-PLL and mPEG-PLGA-PLL-Gal nanoparticles for targeted delivery to hepatomas. *Biomaterials*, 35(2), 760–770.
30. Lv, H., Zhang, S., Wang, B., Cui, S., & Yan, J. (2006). Toxicity of cationic lipids and cationic polymers in gene delivery. *Journal of Controlled Release*, 114(1), 100–109.
31. Ahn, H. H., Lee, J. H., et al. (2008). Polyethyleneimine-mediated gene delivery into human adipose derived stem cells. *Biomaterials*, 29(15), 2415–2422.
32. Hobel, S., Prinz, R., et al. (2008). Polyethylenimine PEI F25-LMW allows the long-term storage of frozen complexes as fully active reagents in siRNA-mediated gene targeting and DNA delivery. *European Journal of Pharmaceutics and Biopharmaceutics*, 70(1), 29–41.
33. Behr, J. P. (1997). The proton sponge: A trick to enter cells the viruses did not exploit. *Chimia*, 51(1–2), 34–36.
34. Dong, X., Tian, H. Y., Chen, L., Chen, J., & Chen, X. S. (2011). Biodegradable mPEG-b-P(MCC-g-OEI) copolymers for efficient gene delivery. *Journal of Controlled Release*, 152(1), 135–142.
35. Endres, T. K., Beck-Broichsitter, M., Samsonova, O., Renette, T., & Kissel, T. H. (2011). Self-assembled biodegradable amphiphilic PEG-PCL-IPEI triblock copolymers at the borderline between micelles and nanoparticles designed for drug and gene delivery. *Biomaterials*, 32(30), 7721–7731.
36. Hatakeyama, H., Akita, H., & Harashima, H. (2011). A multi-functional envelope type nano device (MEND) for gene delivery to tumours based on the EPR effect: A strategy for overcoming the PEG dilemma. *Advanced Drug Delivery Reviews*, 63(3), 152–160.
37. Li, Y., Kroger, M., & Liu, W. K. (2014). Endocytosis of PEGylated nanoparticles accompanied by structural and free energy changes of the grafted polyethylene glycol. *Biomaterials*, 35(30), 8467–8478.
38. Hosseinkhani, H., Hiraoka, Y., et al. (2013). Engineering three-dimensional collagen-IKVAV matrix to mimic neural microenvironment. *ACS Chemical Neuroscience*, 4(8), 1229–1235.
39. Pallarola, D., Bochen, A., et al. (2014). Interface immobilization chemistry of cRGD-based peptides regulates integrin mediated cell adhesion. *Advanced Functional Materials*, 24(7), 943–956.
40. Zhao, F., Yin, H., & Li, J. (2014). Supramolecular self-assembly forming a multifunctional synergistic system for targeted co-delivery of gene and drug. *Biomaterials*, 35(3), 1050–1062.
41. Li, B., Qiu, T., Zhang, P., Wang, X., Yin, Y., & Li, S. (2014). IKVAV regulates ERK1/2 and Akt signalling pathways in BMMSC population growth and proliferation. *Cell Proliferation*, 47(2), 133–145.
42. Singh, S. R., Grossniklaus, H. E., et al. (2009). Intravenous transferrin, RGD peptide and dual-targeted nanoparticles enhance anti-VEGF intraceptor gene delivery to laser-induced CNV. *Gene Therapy*, 16(5), 645–659.
43. Wibowo, A. S., Singh, M., et al. (2013). Structures of human folate receptors reveal biological trafficking states and diversity in folate and antifolate recognition. *Proceedings of the National Academy of Sciences of the United States of America*, 110(38), 15180–15188.
44. Berns, E. J., Sur, S., et al. (2014). Aligned neurite outgrowth and directed cell migration in self-assembled monodomain gels. *Biomaterials*, 35(1), 185–195.
45. Liu, C. (2016). Novel fibrous scaffolds with dual growth factor delivery and non-viral gene delivery for neural tissue engineering. (Thesis). University of Hong Kong.

Publisher's Note Springer Nature remains neutral with regard to jurisdictional claims in published maps and institutional affiliations.